Chapter 5

Modifying Alkylzinc Chemistry with 2, 2′-Dipyridylamide: Activation of ^{t}Bu-Zn Bonds Towards *Para*-Alkylation of Benzophenone

Supporting Information

Table of Contents

Table of Figures

Additional Crystal Information

Table S1 Crystallographic data and refinement details for compounds **18**-**21**.

Compound	**18**	**19**	**20**	**21**
Empirical formula	$C_{28}H_{34}N_6Zn_2$	$C_{40}H_{66}N_{10}Na_2Zn$	$C_{50}H_{92}N_3NaO_6Zn_2$	$C_{50}H_{92}KN_3O_6Zn_2$
M_r (g mol^{-1})	585.35	798.38	985.00	1001.11
Crystal system	Monoclinic	Monoclinic	Triclinic	Triclinic
Space group	$P2_1/c$	$P2_1/n$	P -1	P-1
a/ Å	9.4833(3)	11.5137(3)	10.0075(11)	9.8787(6)
b/ Å	10.4377(4)	21.6403(4)	11.1283(9)	11.2247(7)
c/ Å	14.0888(5)	18.3837(3)	13.3084(15)	13.5206(7)
α (º)	90	90	69.353(9)	72.296(5)
β (º)	105.844(4)	93.636(2)	85.491(9)	83.032(5)
γ (º)	90	90	84.723(8)	84.558(5)
V/Å^3	1341.58(8)	4571.26(16)	1379.3(2)	1415.02(14)
Z	2	4	1	1
2θmax	58.0	57.9	58.0	60.4
Measured reflections	7483	23176	16565	15934
Unique reflections	3451	10516	6820	7408
R_{int}	0.0284	0.0243	0.0346	0.0309
Observed rflns [$I > 2\sigma(I)$]	2840	8121	5614	5590
μ (mm^{-1})	1.816	0.594	0.922	0.965
No. of parameters	166	492	321	359
R [on *F*, obs rflns only]	0.0413	0.0388	0.0606	0.0642
wR [on F^2, all data]	0.1039	0.0864	0.1679	0.1874
GoF	1.065	1.032	1.057	1.034
Largest diff. peak/hole/e Å^{-3}	1.583/-0.732	0.549/-0.494	0.912/-0.723	0.911/-0.597

NMR Spectra

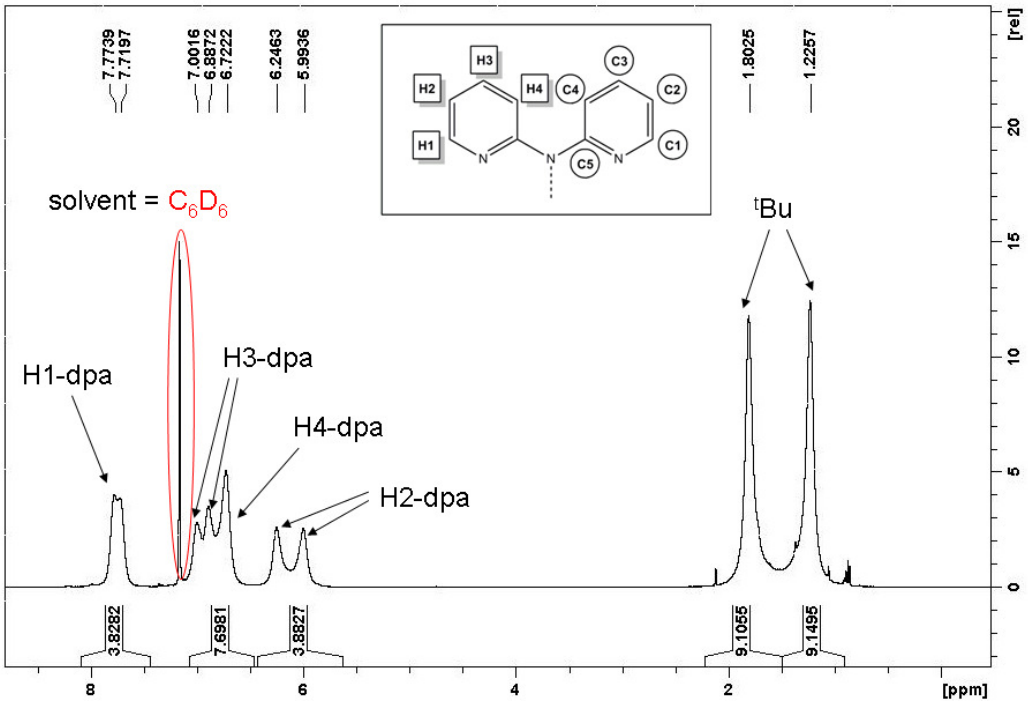

Figure S1 ^{1}H NMR Spectrum of [{(dpa)Zn(^{t}Bu)}$_2$] (**18**).

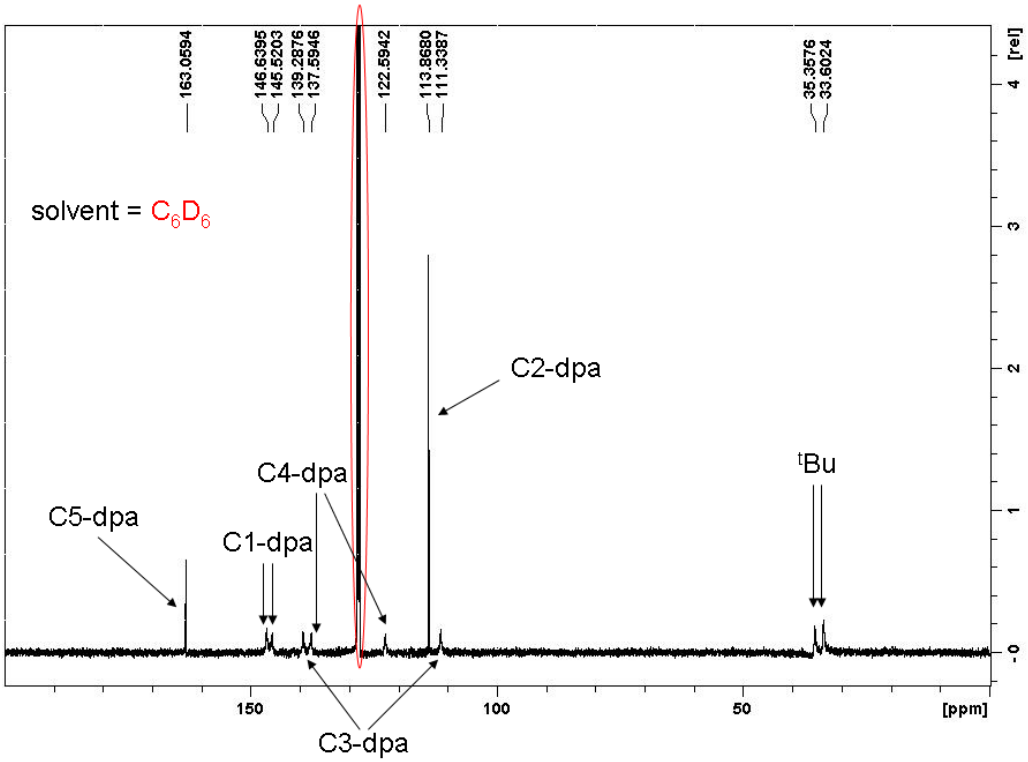

Figure S2 ^{13}C NMR Spectrum of [{(dpa)Zn(^{t}Bu)}$_2$] (**18**).

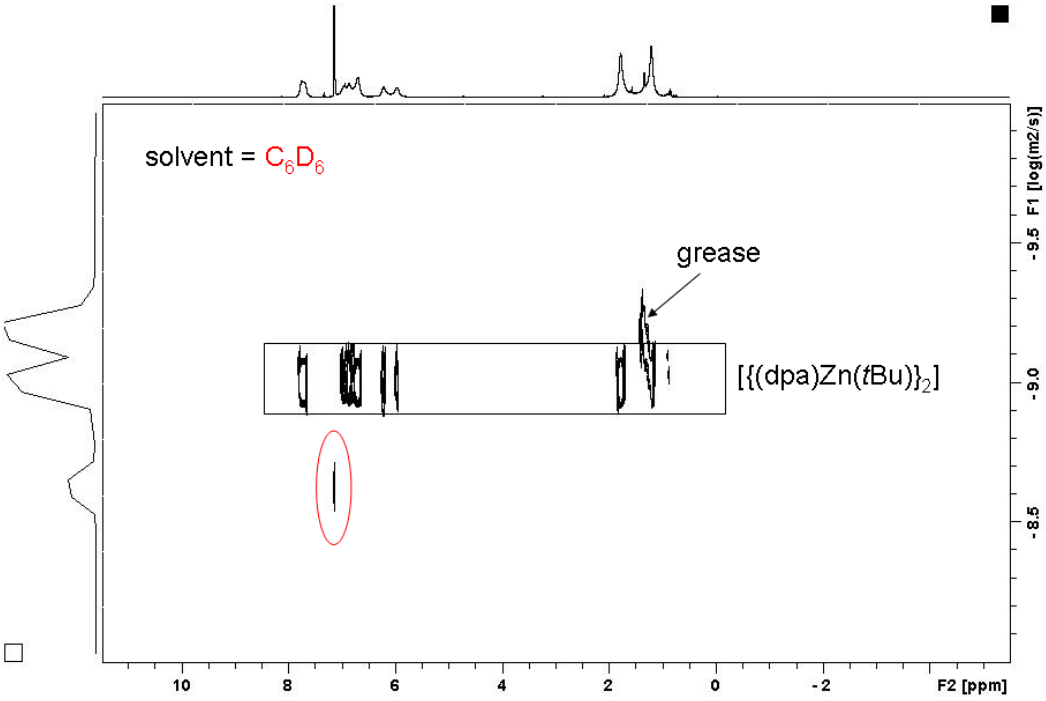

Figure S3 DOSY NMR Spectrum of [{(dpa)Zn(^{t}Bu)}$_2$] (**18**).

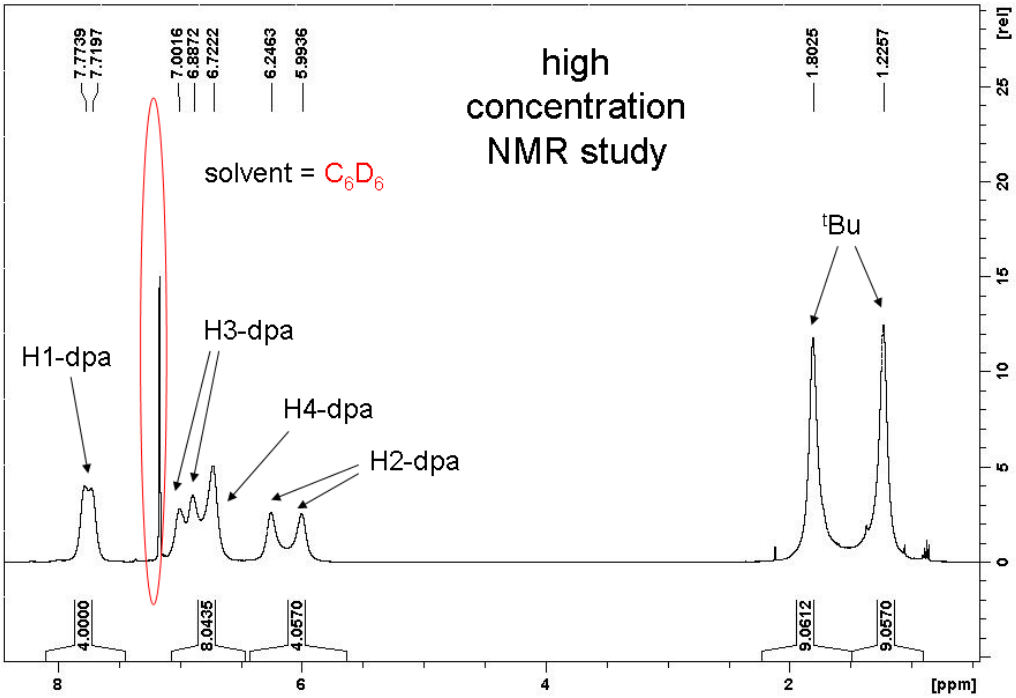

Figure S4 High concentration ^{1}H NMR spectrum of [{(dpa)Zn(^{t}Bu)}$_2$] (**18**).

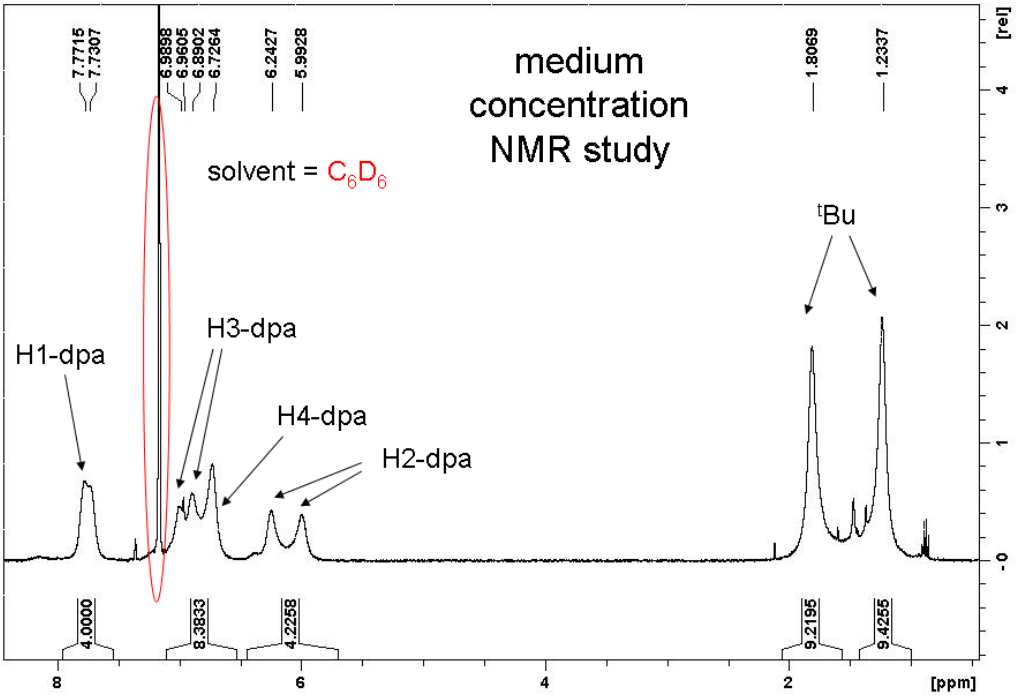

Figure S5 Medium concentration ^{1}H NMR spectrum of [{(dpa)Zn(^{t}Bu)}$_2$] (**18**).

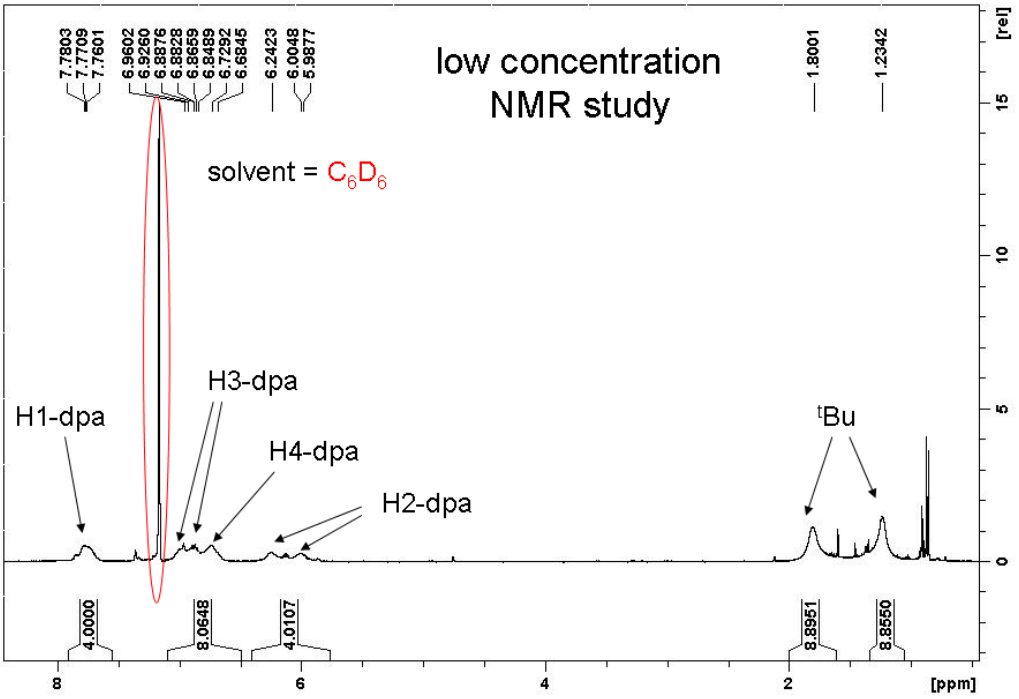

Figure S6 Low concentration ^{1}H NMR spectrum of [{(dpa)Zn(^{t}Bu)}$_2$] (**18**).

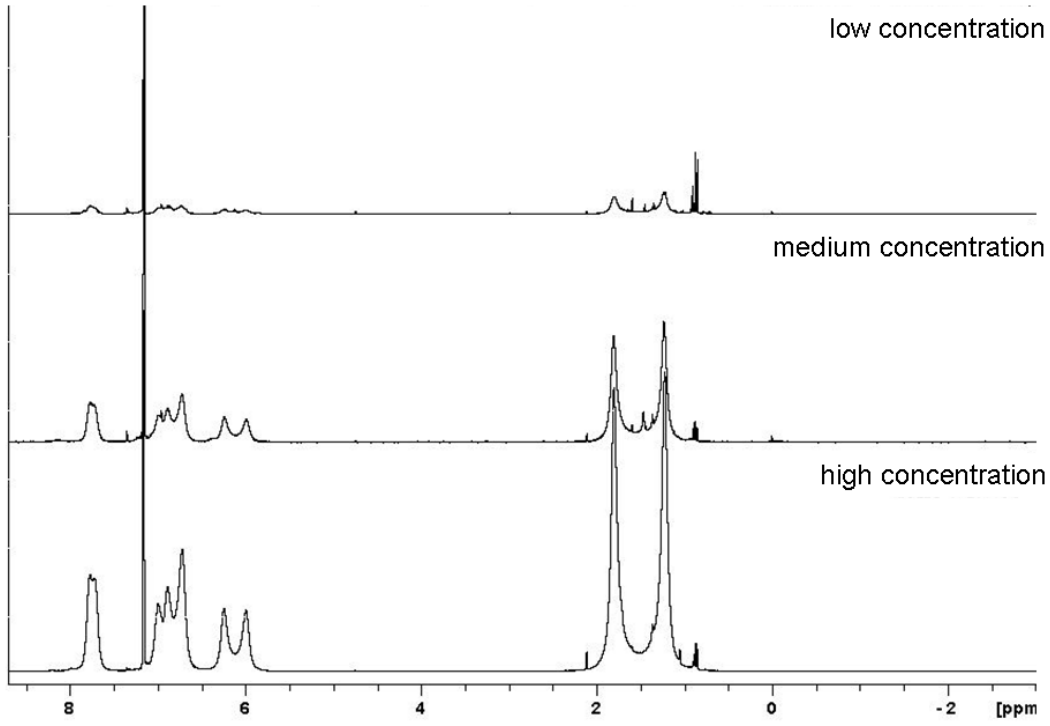

Figure S7 Variable concentration ^{1}H NMR spectra of [{(dpa)Zn(^{t}Bu)}$_2$] (**18**).

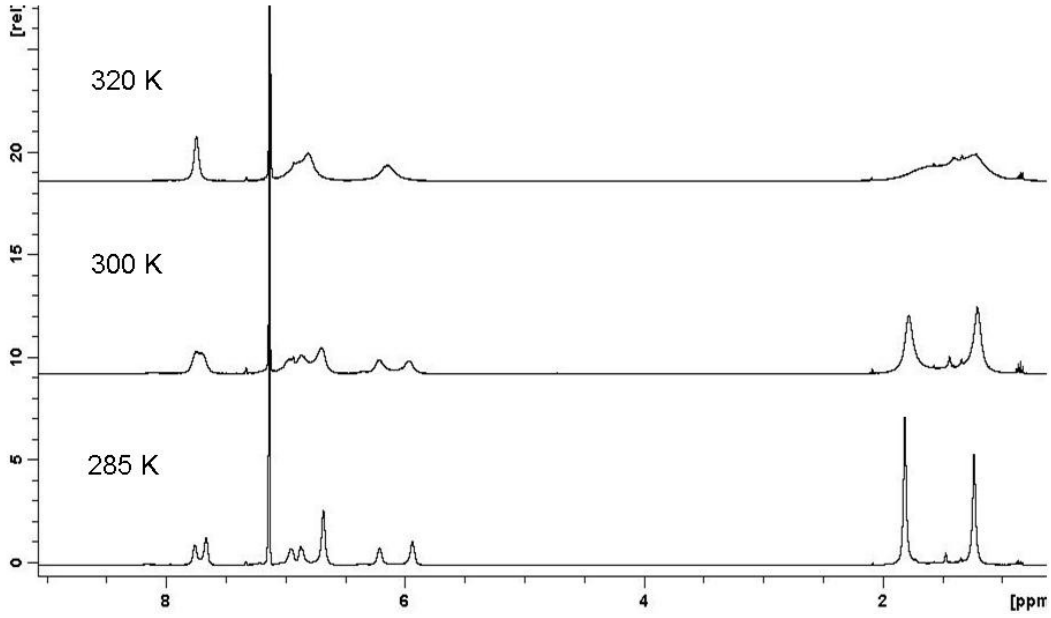

Figure S8 Variable temperature ^{1}H NMR spectra of [{(dpa)Zn(^{t}Bu)}$_2$] (**18**) in C_6D_6 solvent.

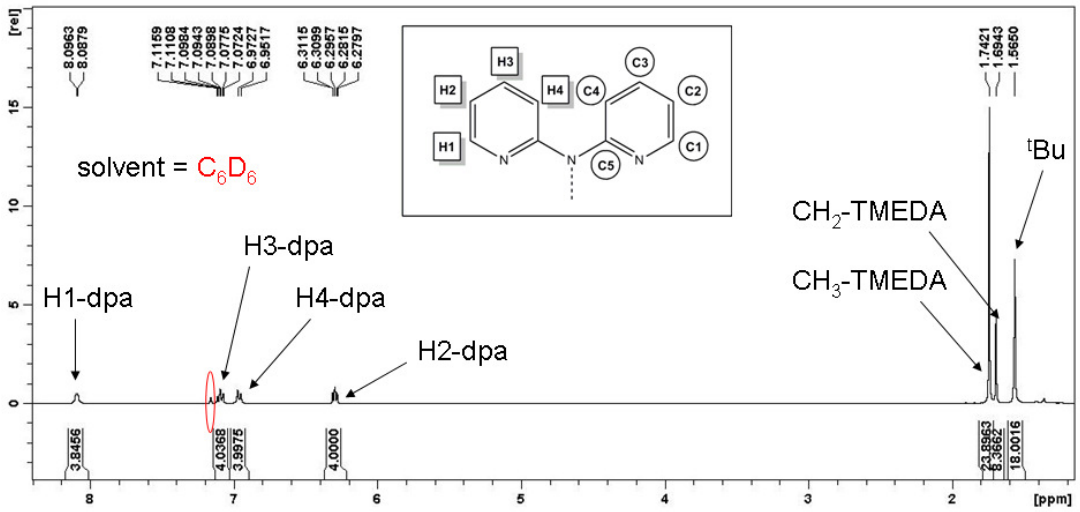

Figure S9 ^{1}H NMR Spectrum of [(TMEDA)$_2$Na$_2$(μ-dpa)$_2$Zn(^{t}Bu)$_2$] (**19**).

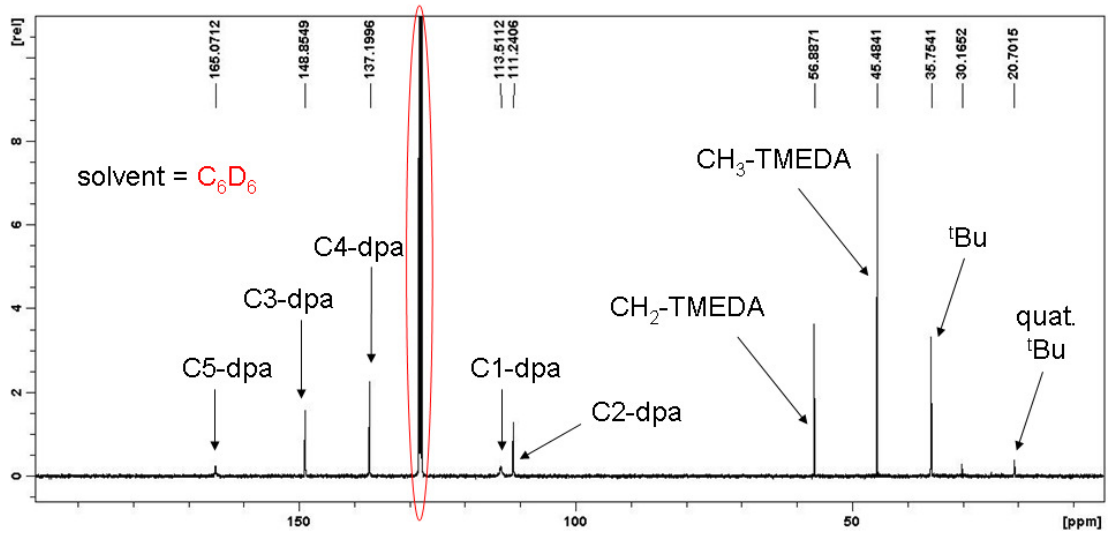

Figure S1 ^{13}C NMR Spectrum of [(TMEDA)$_2$Na$_2$(μ-dpa)$_2$Zn(^{t}Bu)$_2$] (**19**).

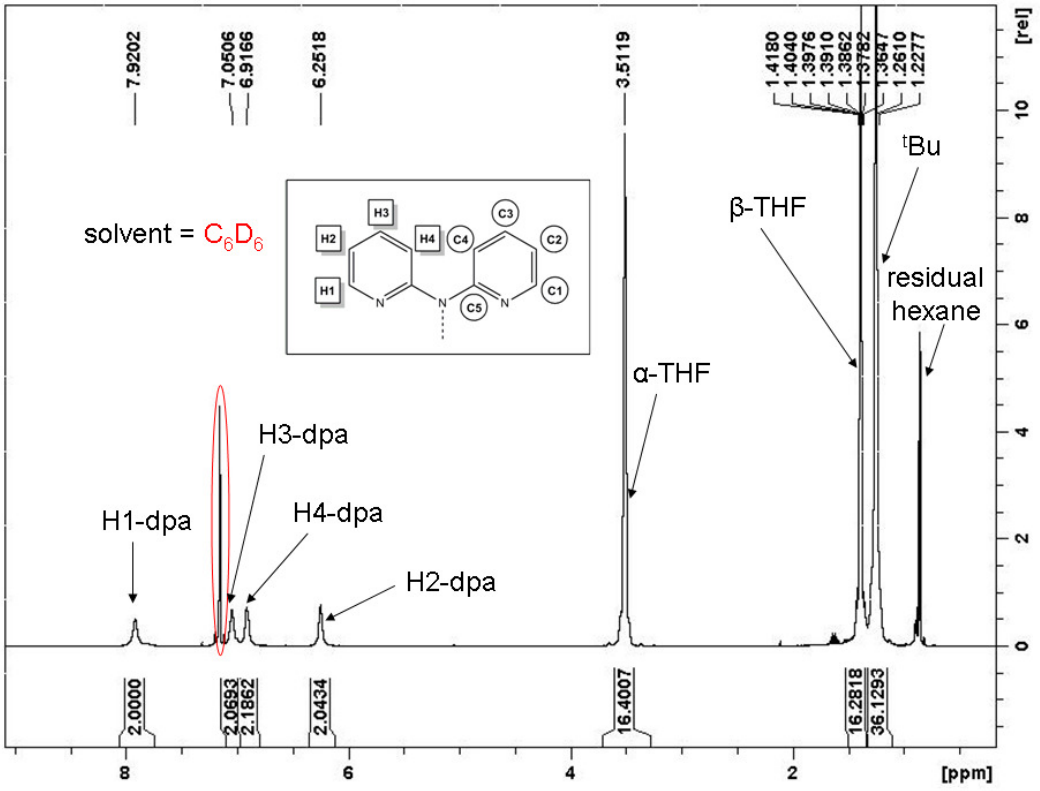

Figure S2 ^{1}H NMR Spectrum of [{Na(THF)$_6$}$^+${Zn(^{t}Bu)$_2$(dpa)Zn(^{t}Bu)$_2$}$^-$] (**20**).

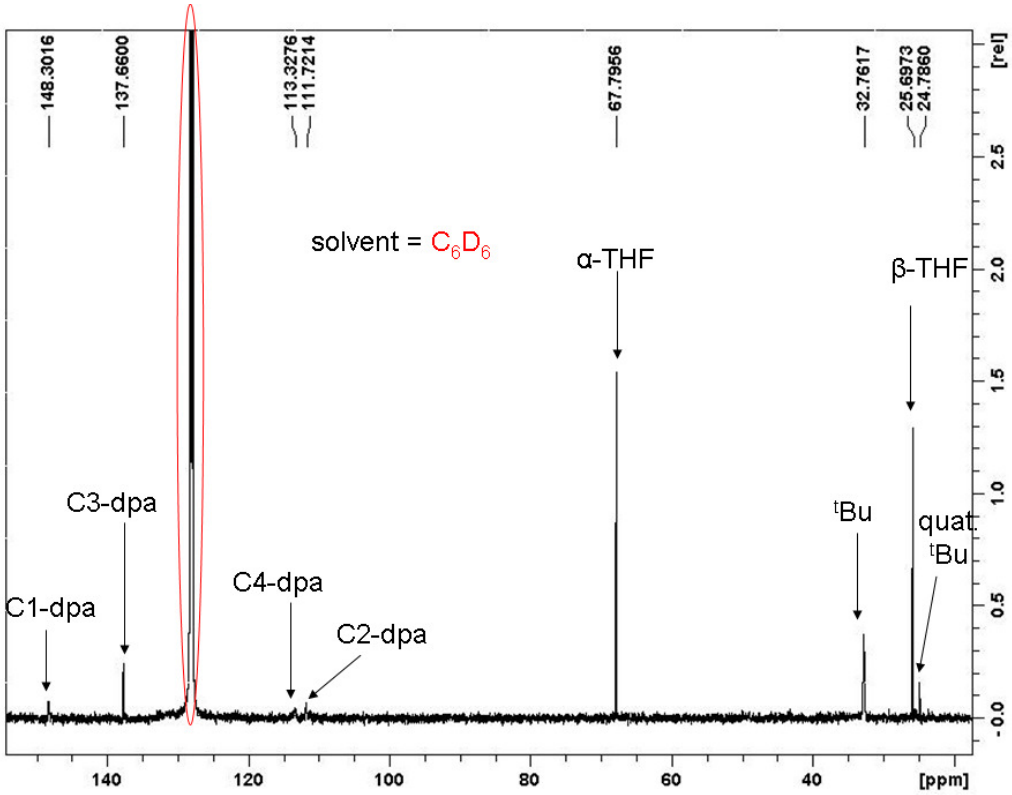

Figure S12 ^{13}C NMR Spectrum of [{Na(THF)$_6$}$^+${Zn(^{t}Bu)$_2$(dpa)Zn(^{t}Bu)$_2$}$^-$] (**20**).

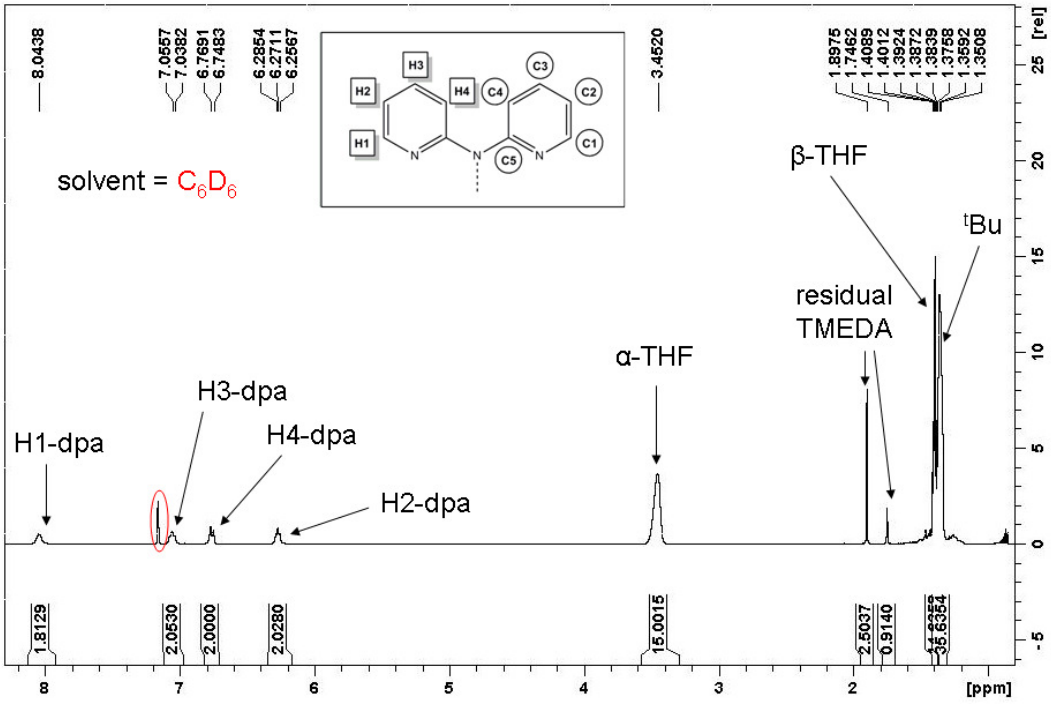

Figure S13 ^{1}H NMR Spectrum of [{K(THF)$_6$}$^+${Zn(^{t}Bu)$_2$(dpa)Zn(^{t}Bu)$_2$}$^-$] (**21**).

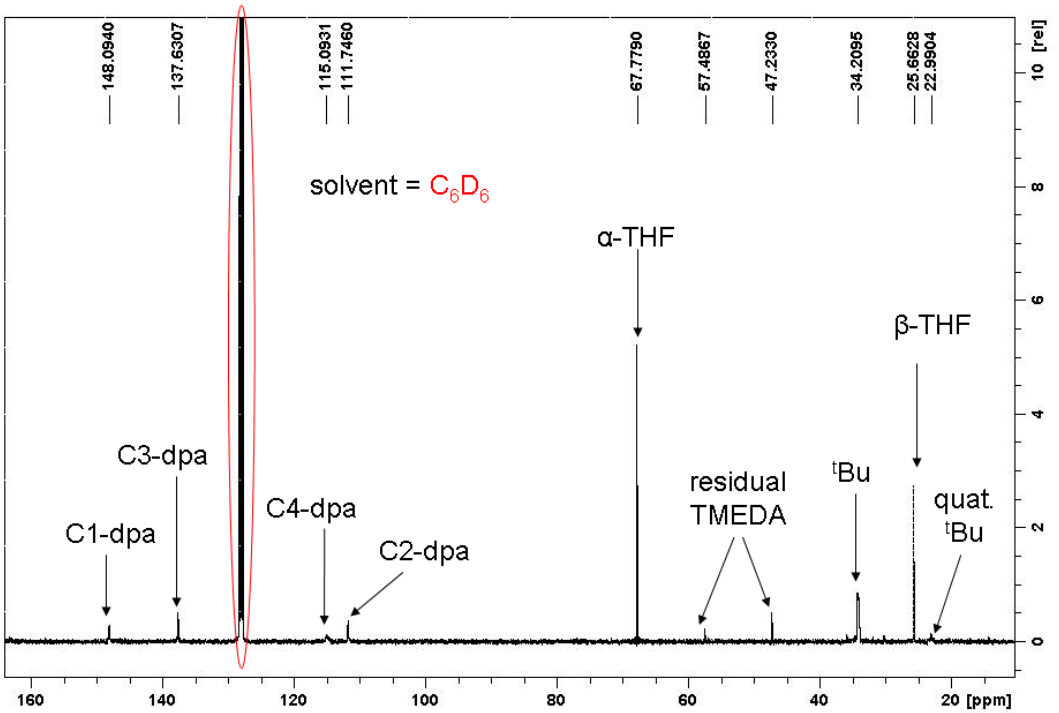

Figure S14 ^{13}C NMR Spectrum of [{K(THF)$_6$}$^+${Zn(^{t}Bu)$_2$(dpa)Zn(^{t}Bu)$_2$}$^-$] (**21**).

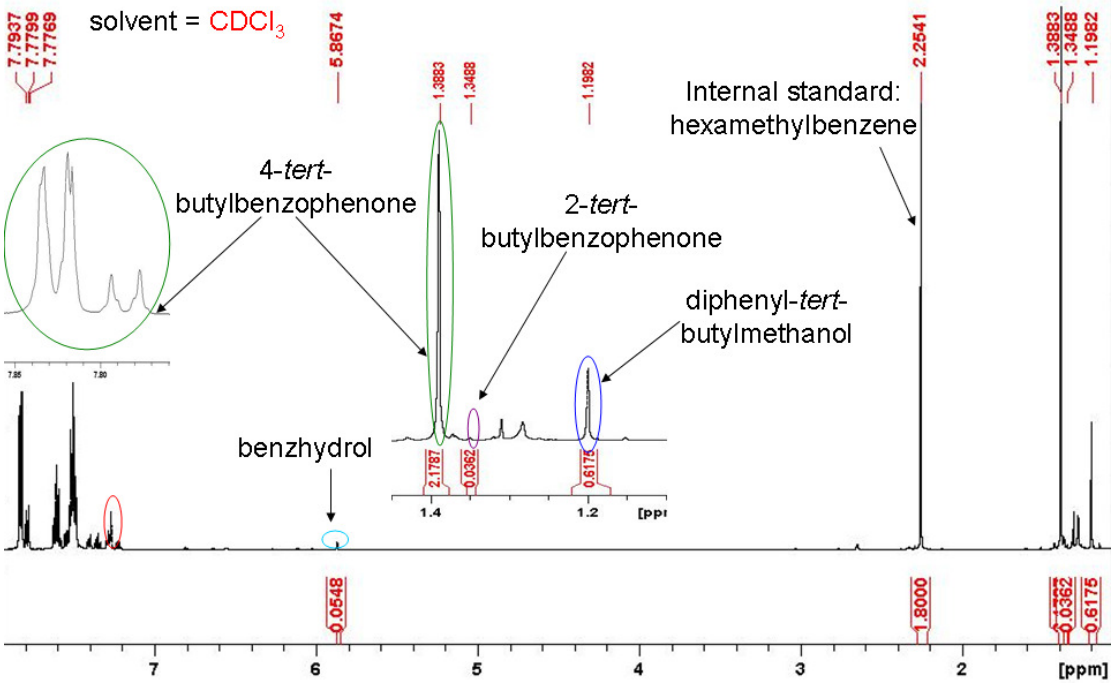

Figure S3 Crude NMR Spectrum of 4-tert-butylbenzophenone and additional by-products.

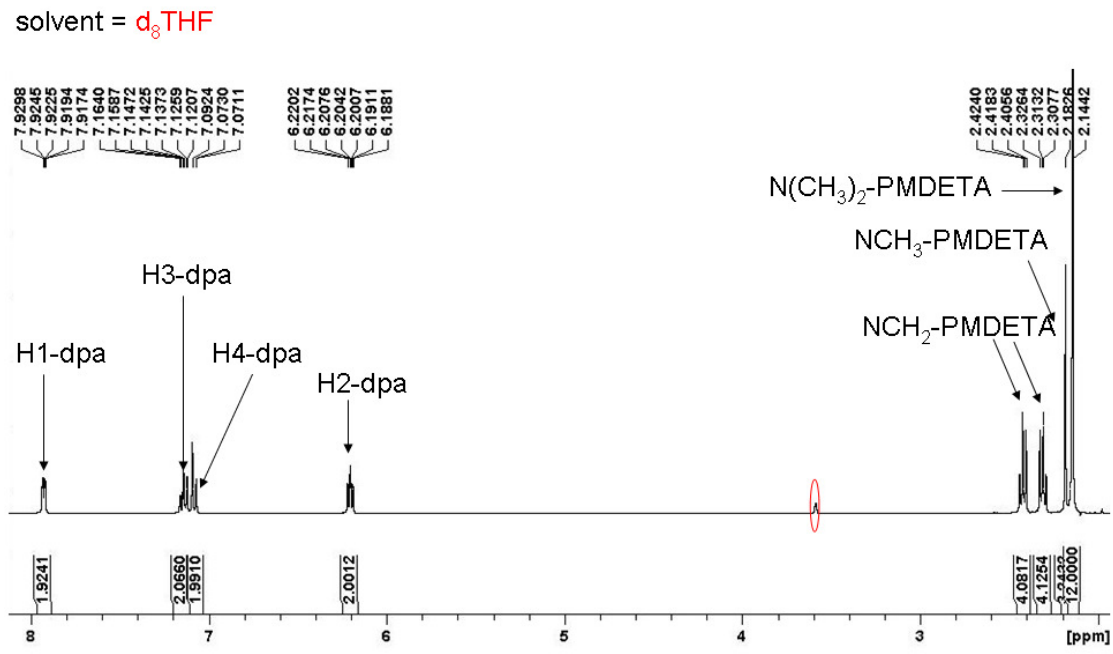

Figure S4 ^{1}H NMR Spectrum of $[(PMDETA)Na(dpa)]_2$, (**22**).

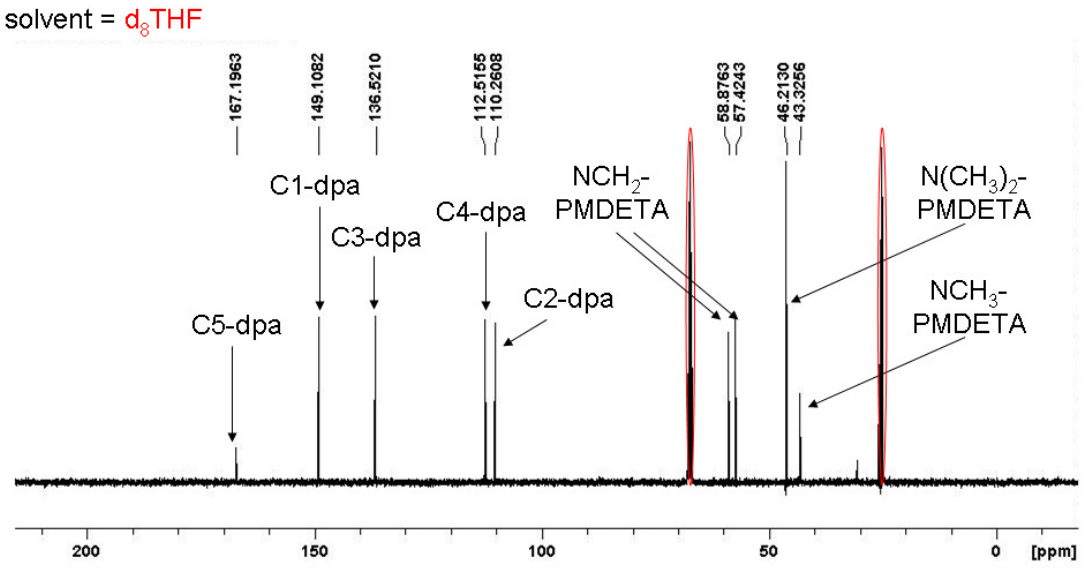

Figure S5 ^{13}C NMR Spectrum of [(PMDETA)Na(dpa)]$_2$, (**22**)**.**

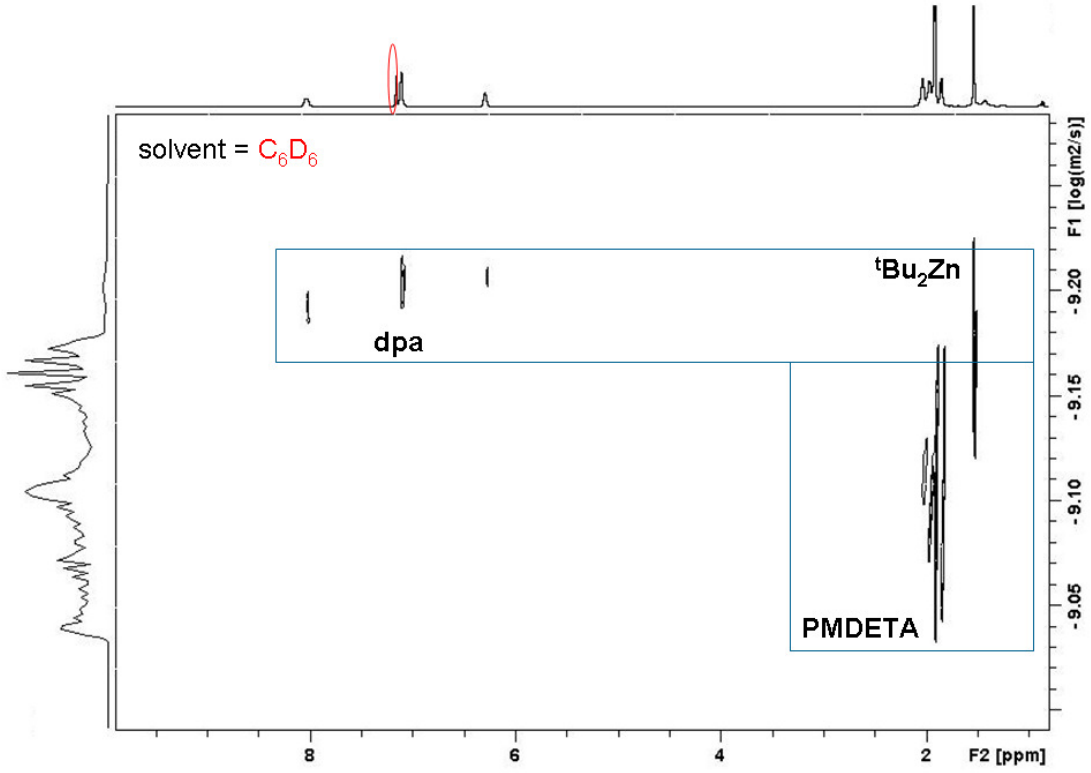

Figure S18 DOSY NMR Spectrum of [(PMDETA)Na(dpa)]$_2$, (**22**) with ^{t}Bu$_2$Zn.

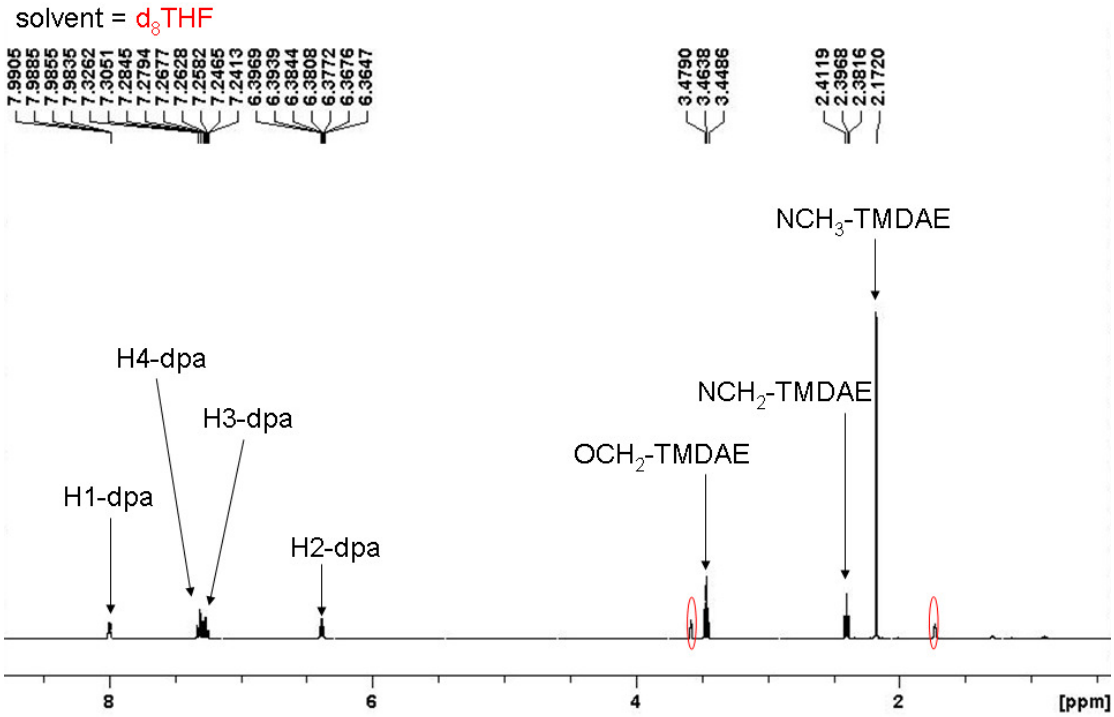

Figure S19 ^{1}H NMR Spectrum of [(TMDAE)Na(dpa)]$_2$, (**23**).

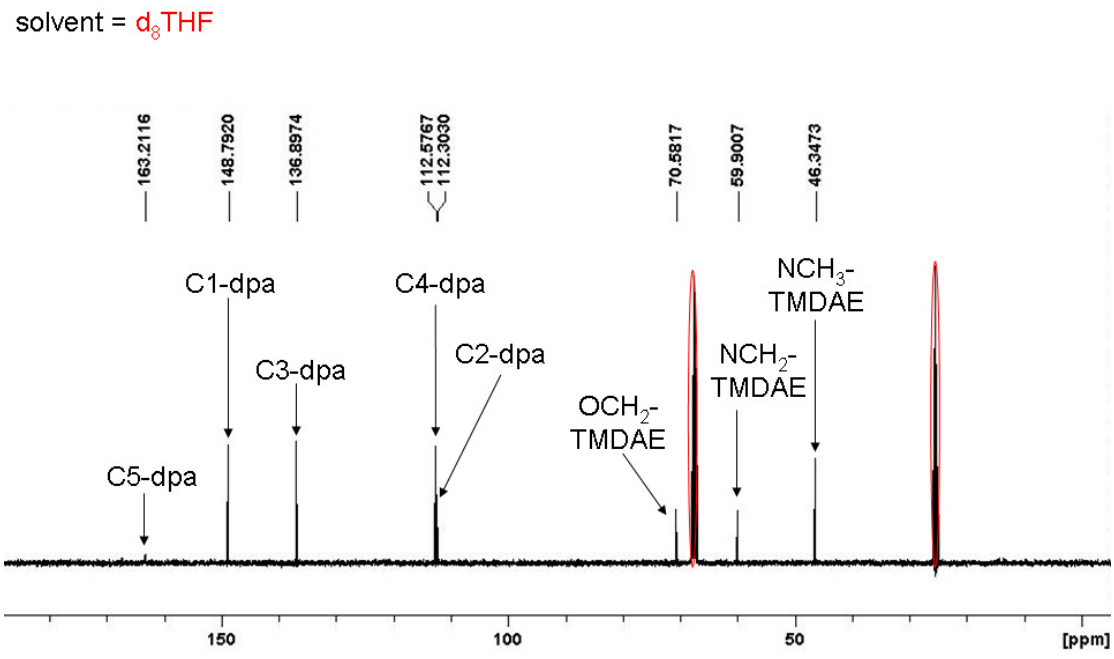

Figure S20 ^{13}C NMR Spectrum of [(TMDAE)Na(dpa)]$_2$, (**23**).

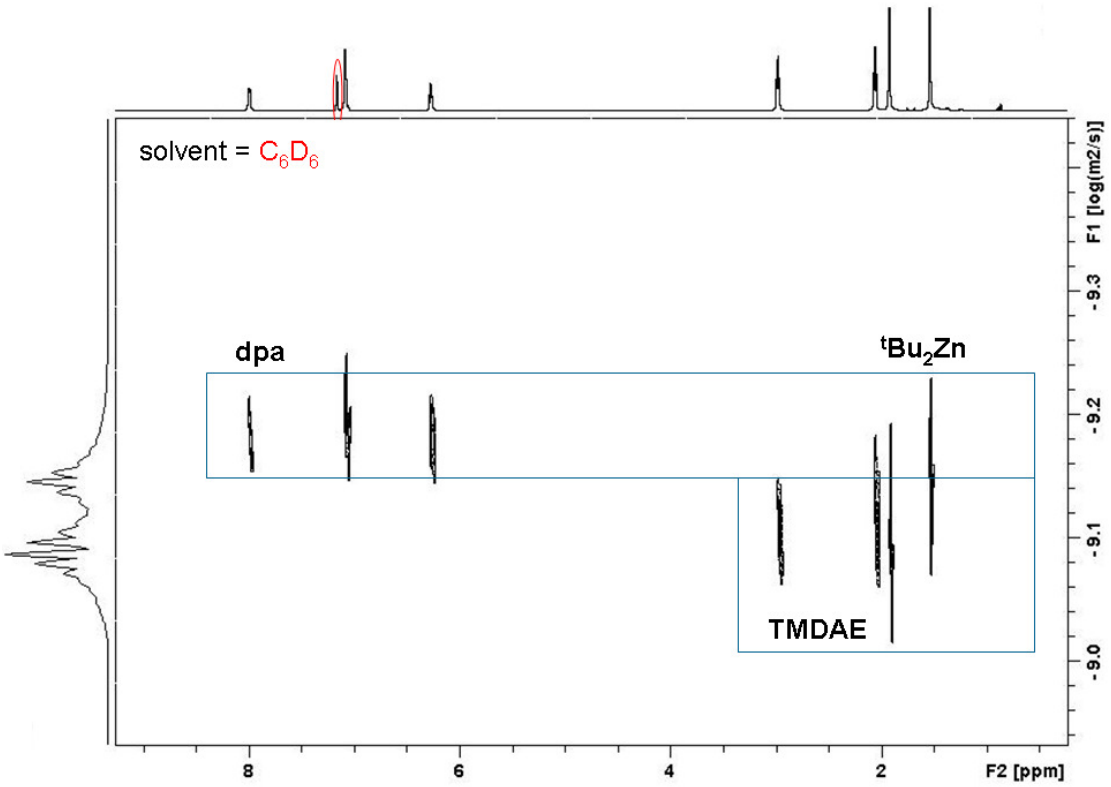

Figure S21 DOSY NMR Spectrum of $[(TMDAE)Na(dpa)]_2$, (**23**) with $^tBu_2Zn$.

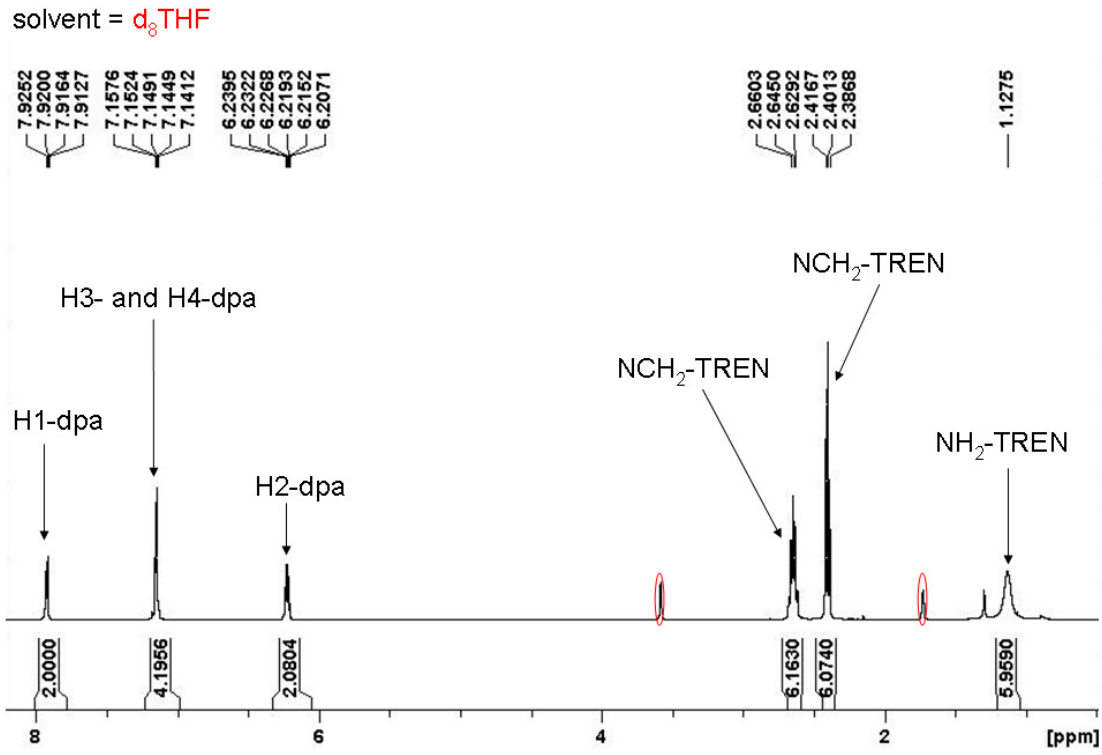

Figure S22 ^{1}H NMR Spectrum of $[(H_6\text{-TREN})Na(dpa)]$, (**24**).

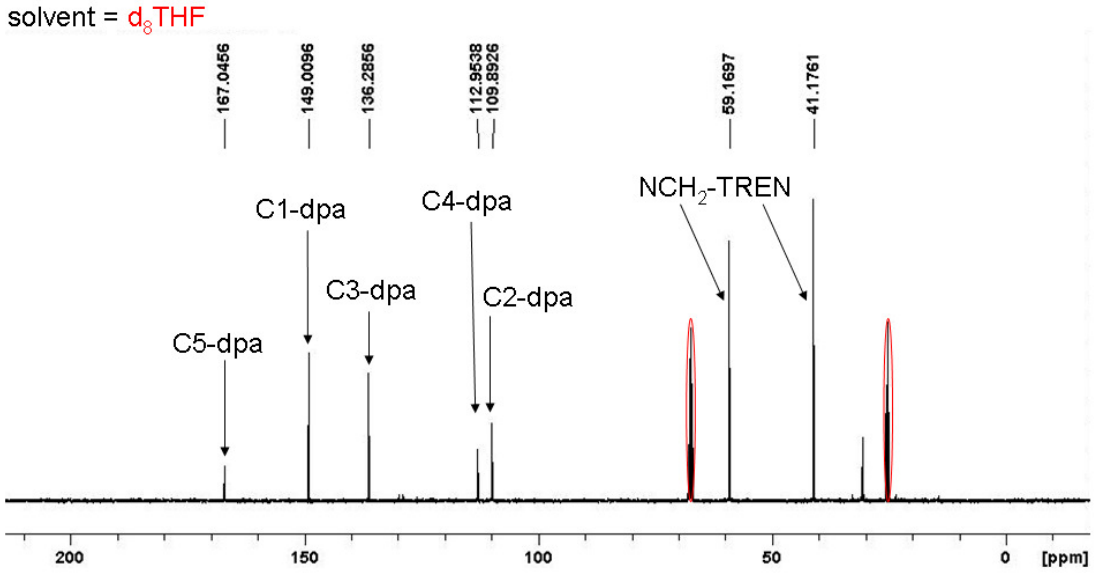

Figure S23 ^{13}C NMR Spectrum of [(H_6-TREN)Na(dpa)], (**24**).

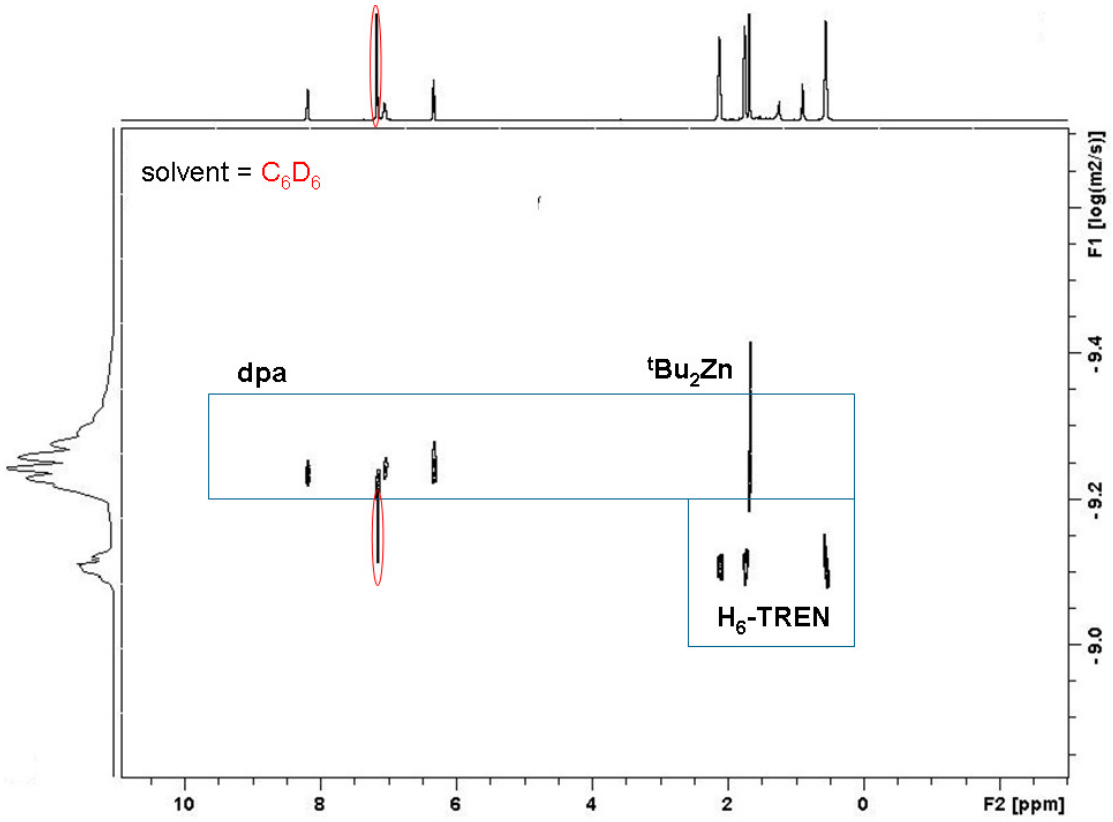

Figure S24 DOSY NMR Spectrum of [(H_6-TREN)Na(dpa)], (**24**) with $^{t}Bu_2Zn$.

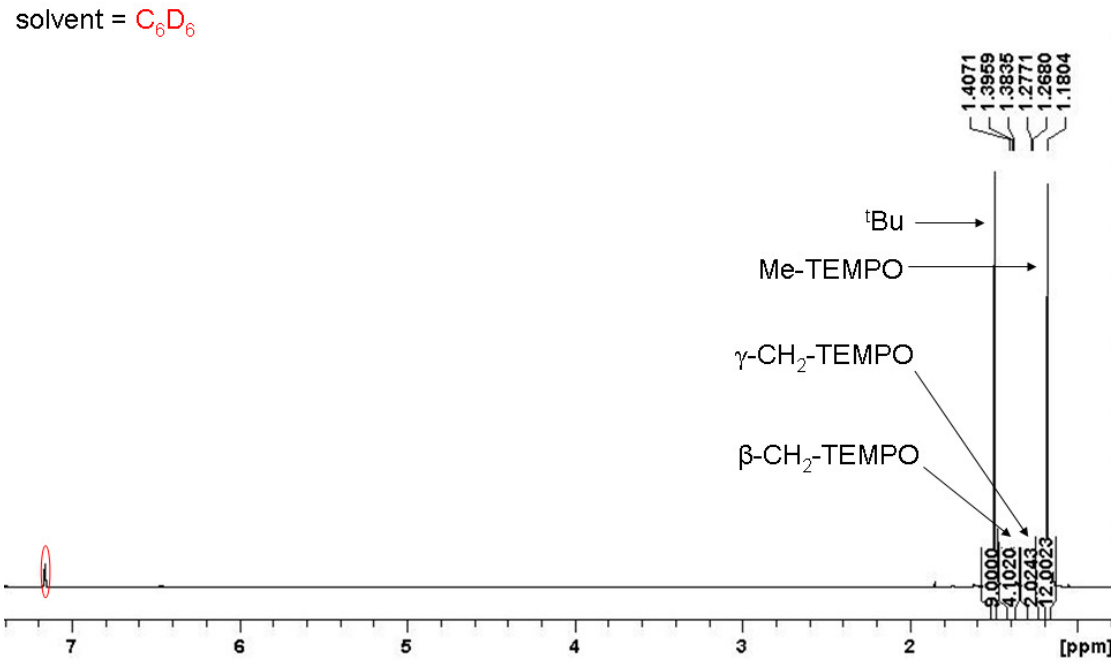

Figure S25 ^{1}H NMR Spectrum of [(TEMPO)Zn(^{t}Bu)].

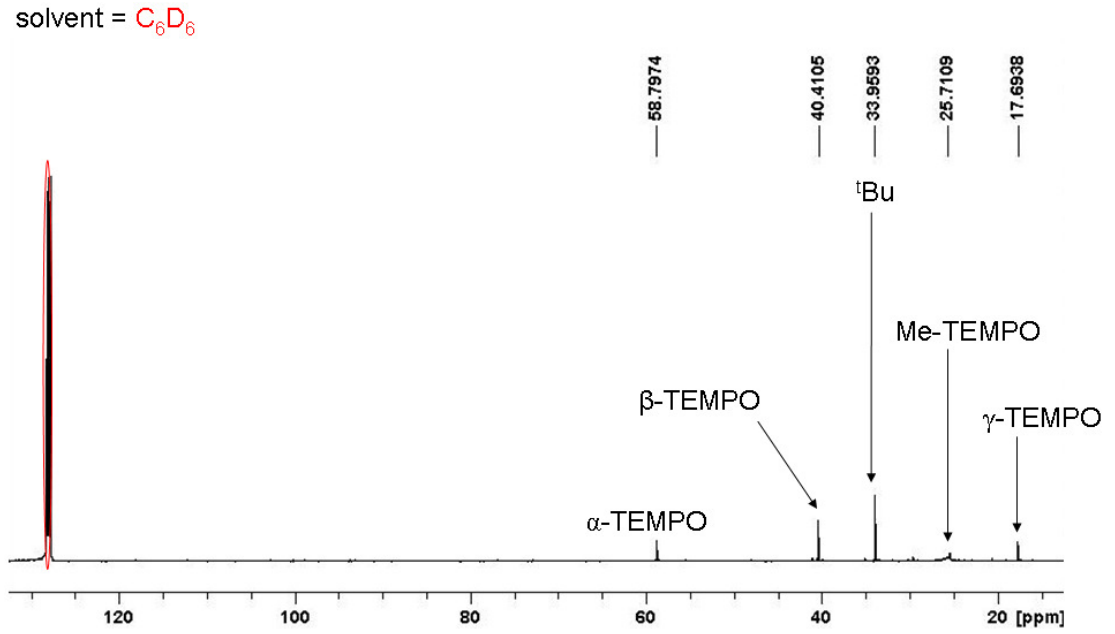

Figure S26 ^{13}C NMR Spectrum of [(TEMPO)Zn(^{t}Bu)].

DOSY and Variable Temperature NMR Spectroscopic Analysis of 18, 22, 23 and 24

The Diffusion-Ordered Spectroscopy (DOSY) NMR experiments were performed on a Bruker AVANCE 400 NMR spectrometer operating at 400.13 MHz for proton resonance under TopSpin (version 2.0, Bruker Biospin, Karlsruhe) and equipped with a BBFO-z-atm probe with actively shielded z-gradient coil capable of delivering a maximum gradient strength of 54 G/cm. Diffusion ordered NMR data was acquired using the Bruker pulse program dstegp3s employing a double stimulated echo with three spoiling gradients. Sine-shaped gradient pulses were used with a duration of 3 ms together with a diffusion period of 100 ms. Gradient recovery delays of 200 μs followed the application of each gradient pulse. Data was accumulated by linearly varying the diffusion encoding gradients over a range from 2% to 95% of maximum for 64 gradient increment values. DOSY plot was generated by use of the DOSY processing module of TopSpin. Parameters were optimized empirically to find the best quality of data for presentation purposes.

At ambient temperature, ^{1}H and ^{13}C NMR spectra of **18** in C_6D_6 solution display two sets of pyridyl resonances and two *t*Bu resonances (Figure S3 and Figure S4), where one set may be expected due to the centre of symmetry of **1** in the solid state. Variable temperature ^{1}H NMR analysis revealed that these resonances coalesce at 320K, whilst cooling to subambient temperature enhances their separation. A variable concentration study (Figure S4 - S7), alongside a DOSY NMR spectrum (Figure S3), suggest the two sets of resonances belong to the same species, hence this effect is likely to be a result of conformational isomerism as opposed to any dimer/monomer equilibrium (refer to DFT calculations for further information).

Table S2 Diffusion coefficients obtained from ^{1}H DOSY NMR experiment for [{(dpa)Zn(^{t}Bu)}$_2$], **18**.

Chemical Shift (ppm)	Peak Assignment	Diffusion Co-efficient D (10^{-10}) m^2 s^{-1}
7.73	H1-dpa	0.545
6.86	H3-dpa	1.007
6.70	H4-dpa	0.782
6.22	H2-dpa	0.657
1.79	*t*Bu	0.782
1.21	*t*Bu	0.840

Table S3 Diffusion coefficients obtained from ^{1}H DOSY NMR experiment for [(PMDETA)Na(dpa)]$_2$, **22** with ^{t}Bu$_2$Zn.

Chemical Shift (ppm)	Peak Assignment	Diffusion Co-efficient D (10^{-10}) m^2 s^{-1}
8.02	H1-dpa	6.354
7.09	H3- and H4-dpa	6.262
6.28	H2-dpa	6.097
2.01	NCH_2-PMDETA	7.681
1.95	NCH_2-PMDETA	8.142
1.89	NCH_3-PMDETA	7.821
1.82	$N(CH_3)_2$-PMDETA	7.515
1.52	*t*Bu	6.856

Table S4 Diffusion coefficients obtained from ^{1}H DOSY NMR experiment for [(TMDAE)Na(dpa)]$_2$, **23** with ^{t}Bu$_2$Zn.

Chemical Shift (ppm)	Peak Assignment	Diffusion Co-efficient D (10^{-10}) m^2 s^{-1}
7.97	H1-dpa	6.661
7.06	H3- and H4-dpa	6.478
6.25	H2-dpa	6.655
2.95	OCH_2-TMDAE	7.864
2.03	NCH_2-TMDAE	7.779
1.90	NCH_3-TMDAE	8.135
1.52	*t*Bu	7.152

Table S5 Diffusion coefficients obtained from ^{1}H DOSY NMR experiment for [(H_6-TREN)Na(dpa)], **24** with $^{t}Bu_2Zn$.

Chemical Shift (ppm)	Peak Assignment	Diffusion Co-efficient D (10^{-10}) m^2 s^{-1}
8.16	H1-dpa	5.912
7.13	H3-dpa	6.159
7.03	H4-dpa	5.632
6.30	H2-dpa	5.766
2.09	NCH_2-TREN	7.839
1.72	NCH_2-TREN	7.759
1.66	*t*Bu	5.580
0.53	NH_2-TREN	7.910

DFT Calculations

DFT calculations were performed using the Gaussian computational package G03.[4] In this series of calculations the B3LYP[5] density functionals and the 6-311G(d,p)[6] basis set were used. After each geometry optimisation, a frequency analysis was performed and the energy values quoted include the zero point energy contribution.

$[(TMEDA)_2Na_2(\mu\text{-}dpa)_2Zn(tBu)_2]$, 19

Dpa Principal Bond Lengths (Å)

N_1-C_2	1.366	1.362
C_2-N_3	1.363	1.365
N_3-C_4	1.338	1.338
C_4-C_5	1.387	1.387
C_5-C_6	1.400	1.400
C_6-C_7	1.381	1.380
C_7-C_2	1.422	1.425
Na_8-N_1	2.582	
Na_8-$N_{3'}$	2.481	
Na_8-N_{10}	2.577	
Na_8-N_{11}	2.624	
Na_8-N_{12}	2.563	
Na_9-N_1	2.521	
Na_9-N_3	2.466	
Na_9-N_{10}	2.550	
Na_8-N_{13}	2.549	
Na_8-N_{14}	2.582	

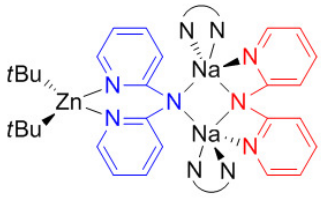

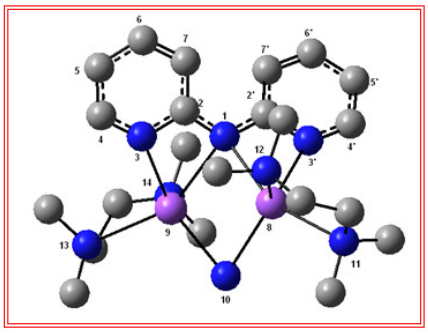

Dpa Principal Bond Angles (˚)

C_2-N_1-$C_{2'}$	122.9
N_1-Na_8-$N_{3'}$	53.9
N_1-Na_9-N_3	54.9
N_1-Na_8-N_{10}	96.9
N_1-Na_9-N_{10}	94.7
Na_8-N_{10}-Na_9	83.7
Na_8-N_1-Na_9	84.2
N_{10}-Na_8-N_{11}	73.5
N_{13}-Na_9-N_{14}	73.4
C_2'-N_1-C_2-C_7	-26.0

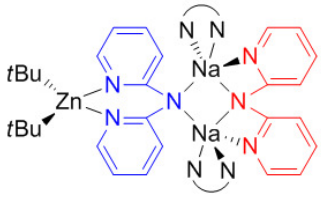

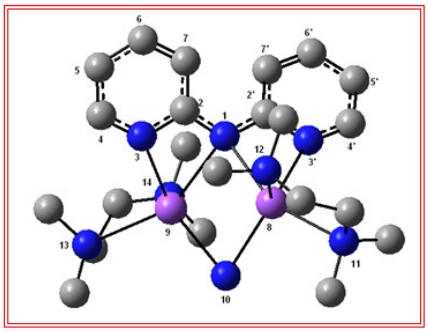

Dpa Principle Bond Indices

N_1-C_2	1.25	1.22
C_2-N_3	1.28	1.29
N_3-C_4	1.40	1.40
C_4-C_5	1.45	1.45
C_5-C_6	1.36	1.37
C_6-C_7	1.51	1.51
C_7-C_2	1.26	1.27
Na_8-N_1	0.02	
Na_8-$N_{3'}$	0.03	
Na_8-N_{10}	0.02	
Na_8-N_{11}	0.02	
Na_8-N_{12}	0.02	
Na_9-N_1	0.02	
Na_9-N_3	0.02	
Na_9-N_{10}	0.02	
Na_8-N_{13}	0.02	
Na_8-N_{14}	0.02	

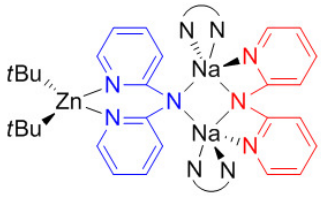

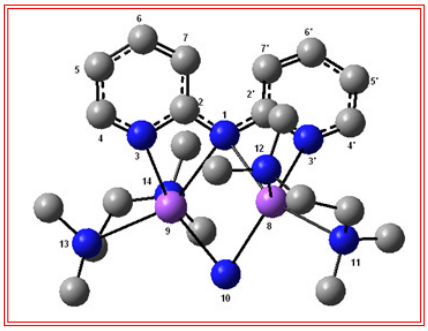

Dpa Charges

N_1	-0.77	
C_2	+0.41	+0.41
N_3	-0.60	-0.60
C_4	+0.08	+0.08
C_5	-0.30	-0.30
C_6	-0.15	-0.15
C_7	-0.31	-0.30
Na_8		+0.88
N_{10}	-0.79	
N_{11}	-0.56	
N_{12}	-0.55	
Na_9		+0.89
N_{13}	-0.55	
N_{14}		-0.56

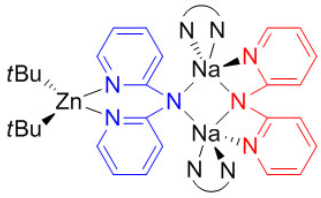

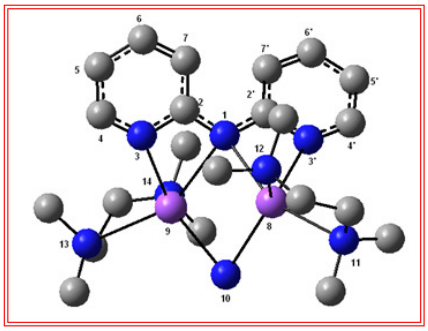

Dpa Principal Bond Lengths (Å) and Angles (˚)

N_{10}-C_2	1.371	1.369
C_2-N_3	1.359	1.360
N_3-C_4	1.346	1.345
C_4-C_5	1.382	1.382
C_5-C_6	1.401	1.400
C_6-C_7	1.377	1.377
C_7-C_2	1.428	1.429
Zn-N_3	2.248	2.252
Zn-C_{15}	2.046	
Zn-C_{16}	2.045	
C_{15}-C_{Me}	1.533, 1.537, 1.536	
C_{16}-C_{Me}	1.533, 1.538, 1.538	
$C_{2''}$-N_{10}-$C_{2'''}$	126.7	
$N_{3''}$–Zn-$N_{3'''}$	80.1	
C_{15}-Zn-C_{16}	134.5	
C_2'-N_1-C_2-C_7	-4.2	

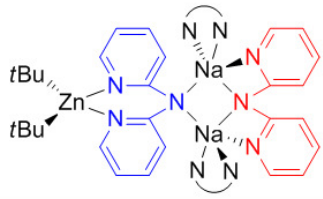

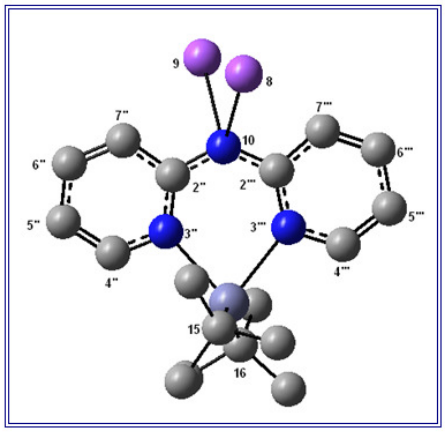

Dpa Principal Bond Indices

N_{10}-C_2	1.23	1.23
C_2-N_3	1.28	1.27
N_3-C_4	1.37	1.36
C_4-C_5	1.47	1.47
C_5-C_6	1.35	1.35
C_6-C_7	1.52	1.52
C_7-C_2	1.27	1.28
Zn-N_3	0.06	0.06
Zn-C_{15}	0.31	
Zn-C_{16}	0.32	
C_{15}-C_{Me}	1.03 1.02 1.02	
C_{16}-C_{Me}	1.03 1.02 1.02	

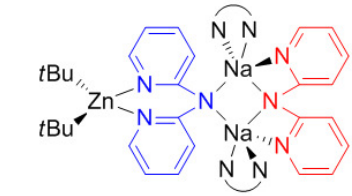

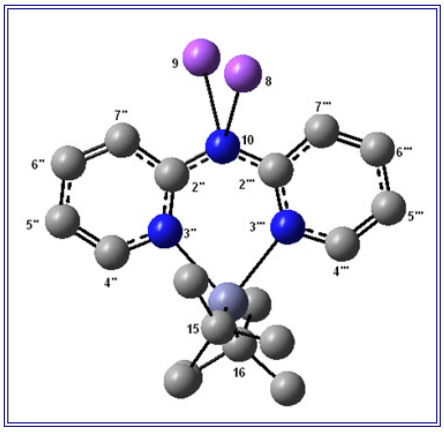

Dpa Charges

N_{10}	-0.79	
C_2	+0.42	+0.42
N_3	-0.63	-0.63
C_4	+0.08	+0.08
C_5	-0.29	-0.29
C_6	-0.16	-0.16
C_7	-0.29	-0.28
Zn	+1.55	
C_{15}	-0.59	
C_{16}	-0.58	
C_{Me}		all -0.59

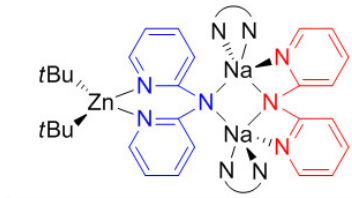

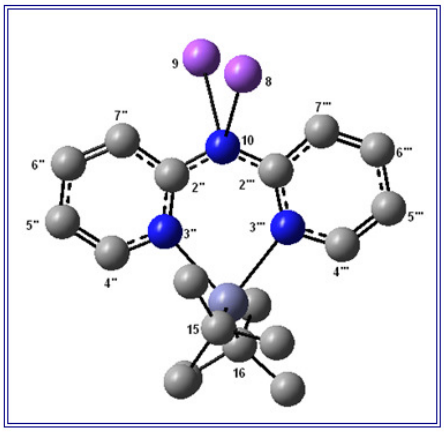

Anion of 20: $[Zn(^tBu)_2(dpa)Zn(^tBu)_2]^-$

Principal Bond Lengths (Å)

N1-C2	1.363	1.363
C2-N3	1.360	1.359
N3-C4	1.345	1.345
C4-C5	1.380	1.380
C5-C6	1.401	1.401
C6-C7	1.374	1.374
C7-C2	1.429	1.428
Zn1-N1	2.206	
Zn2-N3	2.218	2.216
Zn1-C	2.032	2.026
Zn2-C	2.054	2.050

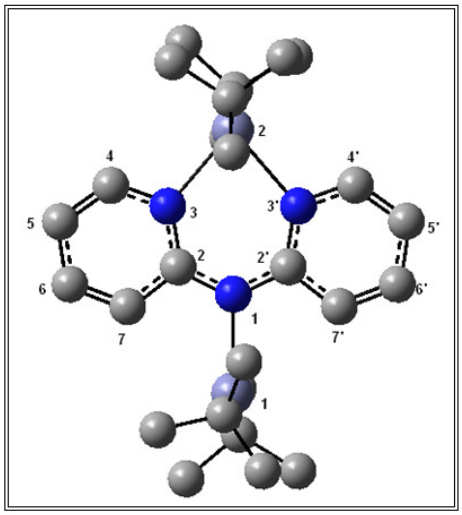

Principal Bond Angles (°)

C_2-N_1-C_2'	127.7
Zn_1-N_1-C_2	116.2 and 115.9
N_3-Zn_2-N_3	81.5
C_2'-N_1-C_2-C_3	1.8

Principal Bond Indices

N1-C2	1.24	1.23
C2-N3	1.27	1.28
N3-C4	1.36	1.36
C4-C5	1.47	1.47
C5-C6	1.34	1.34
C6-C7	1.53	1.53
C7-C2	1.26	1.26
Zn1-N1	0.09	
Zn2-N3	0.06	0.06
Zn1-C	0.34	0.35
Zn2-C	0.30	0.30
C(*t*Bu)-C(Me)	All twelve are 1.03	

Charges

N1	-0.76	
C2	+1.44	+1.44
N3	-0.64	-0.63
C4	+0.08	+0.08
C5	-0.30	-0.30
C6	-0.16	-0.16
C7	-0.26	-0.26
Zn1	+1.47	
Zn2	+1.56	
C(*t*Bu)(Zn1)	-0.57	-0.57
C(*t*Bu)(Zn2)	-0.58	-0.58
C(Me)	All twelve are -0.59	

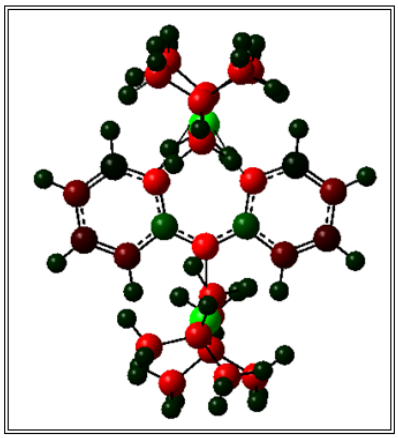

[(PMDETA)Na(dpa)]$_2$, 22

Principal Bond Lengths (Å)

Na1-N1	2.541	N1-C1	1.363
Na1-N2	2.511	N2-C1	1.364
Na1-N3	2.704	N2-C5	1.335
Na1-N4	2.451	C1-C2	1.424
Na1-N5	2.877	C2-C3	1.382
Na1-N6	2.612	C3-C4	1.399
		C4-C5	1.389

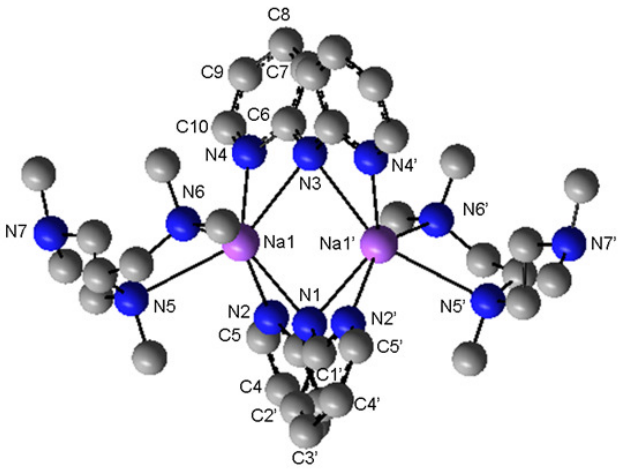

N3-C6	1.362
N4-C6	1.365
N4-C10	1.337
C6-C7	1.426
C7-C8	1.380
C8-C9	1.400
C9-C10	1.387

Principal Bond Angles (˚)

N1-Na1-N2	54.0
N3-Na1-N4	52.9
N5-Na1-N6	67.8
N1-Na1-N3	98.9
Na1-N1-Na1'	84.0
Na1-N3-Na1'	77.9

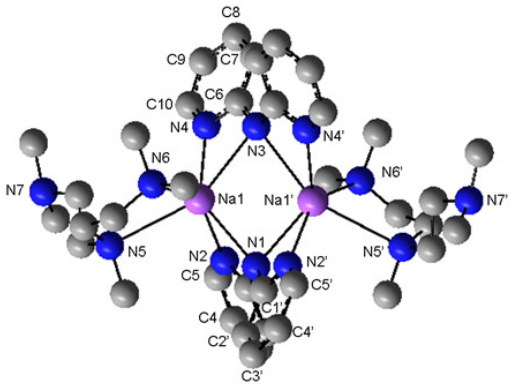

[(H_6-TREN)Na(dpa)], 24

Principal Bond Lengths (Å)

N1-C5	1.353	N1-C6	1.351
N2-C5	1.368	N3-C6	1.373
N2-C1	1.334	N3-C8	1.333
C1-C2	1.389	C9-C10	1.389
C2-C3	1.399	C8-C9	1.400
C3-C4	1.381	C7-C8	1.380
C4-C5	1.427	C6-C7	1.428

Na1-N1	2.388
Na1-N3	2.539
Na1-N6	2.526
Na1-N7	2.510
Na1-N4	2.516
Na1-N5	2.756
C5-N1-C6	126.2
(N4)H…N2	2.068

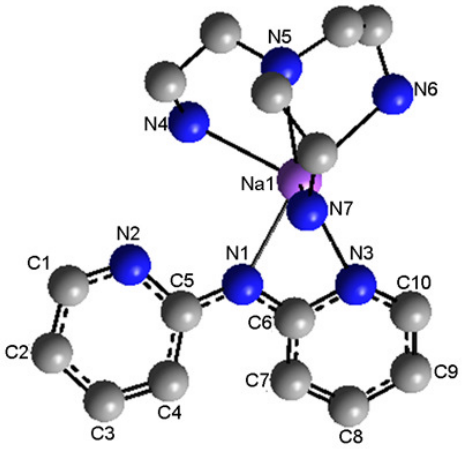

Principal Bond Angles (˚)

N1-Na1-N3	55.1
N4-Na1-N5	69.7
N4-Na1-N6	107.2
N4-Na1-N7	111.8
N5-Na1-N6	69.5
N5-Na1-N7	68.4
N6-Na1-N7	105.3

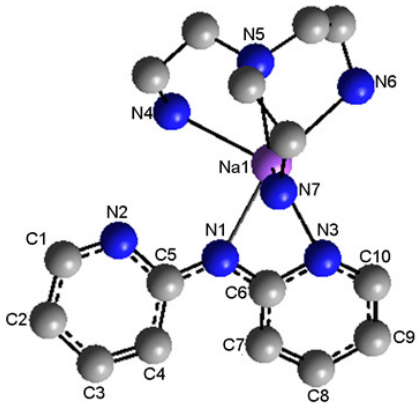

Discussion of Dpa Bond Lengths and Angles

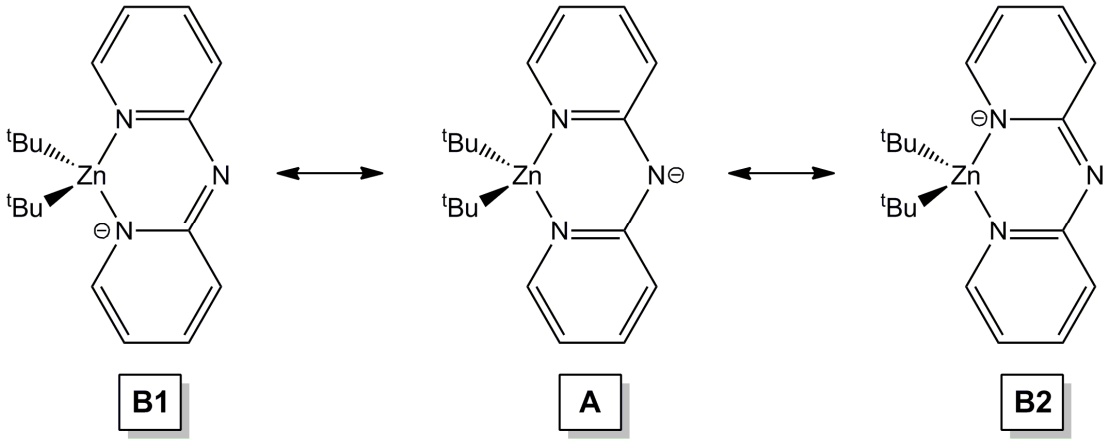

Figure S27 Graphical representation of the resonance delocalisation of dpa.

Through resonance delocalisation, the anionic charge may be focused at the (amido)-N or the (pyridyl)-N (Figure S27). If the anion predominantly lies on the (pyridyl)-N (Figure S27B), this results in a shortened (amido)N-C bond, and elongated (pyridyl)N-C bonds due to the loss of aromaticity. Within Cotton's cobalt complex $[Co(dpa)_2]$,[8] the anionic charge is thought to lie primarily on the (pyridyl)-N, as indicated by the shortened C-(amido)N bond lengths [1.346(4) and 1.344(4) Å] and elongated C-(pyridyl)N bonds [1.367(4) and 1.371(4) Å] (Table S6), in comparison to those of the related compound $[Co\{dpa(H)\}Cl_2]$, with C-(amino)N bond lengths of [1.373(4) and 1.382(4) Å and C-(pyridyl)N bonds of 1.351(4) and 1.348(4) Å].

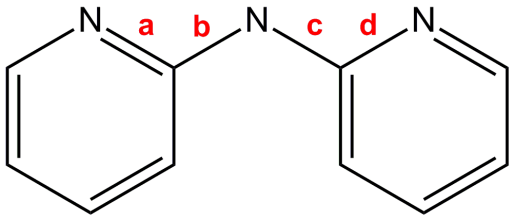

Table S6 Key bond lengths for a range of neutral and anionic dpa complexes.

Compound		Bond Length (Å)			
		a	**b**	**c**	**d**
dpa(H) monoclinic	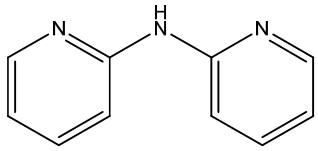	1.343(2)	1.388(2)	1.391(2)	1.335(2)
dpa(H) orthorhombic[9]		1.332(4)	1.379(4)	1.380(4)	1.338(4)
dpa(H) triclinic[10]		1.337(2)	1.380(3)	1.376(3)	1.334(3)
$[Co\{dpa(H)\}Cl_2]$[8]	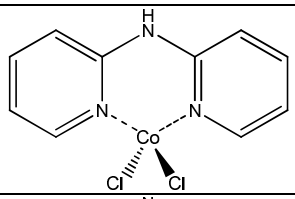	1.351(4)	1.373(4)	1.382(4)	1.348(4)
$[Co(dpa)_2]$[8]	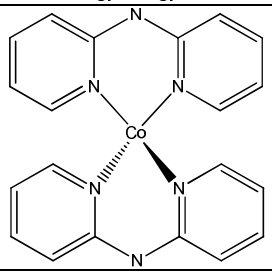	1.367(4)	1.346(4)	1.344(4)	1.371(4)
19	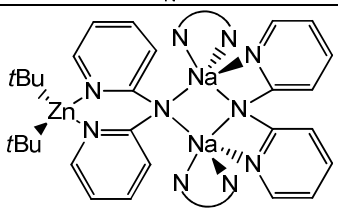	1.347(2)	1.371(2)	1.373(2)	1.346(2)

References

[1] C. Schade, W. Bauer, P. v. R. Schleyer, *J. Organomet. Chem.* **1985**, *295*, C25-C28.

[2] B. Conway, D. V. Graham, E. Hevia, A. R. Kennedy, J. Klett, *Chem. Commun.* **2008**, 2638-2640.

[3] P. C. Andrikopoulos, D. R. Armstrong, H. R. L. Barley, W. Clegg, S. H. Dale, E. Hevia, G. W. Honeyman, A. R. Kennedy, R. E. Mulvey, *J. Am. Chem. Soc* **2005**, *127*, 6184-6185.

[4] M. J. Frisch, G. W. Trucks, H. B. Schlegel, G. E. Scuseria, M. A. Robb, J. R. Cheeseman, J. A. Montgomery, Jr., T. Vreven, K. N. Kudin, J. C. Burant, J. M. Millam, S. S. Iyengar, J. Tomasi, V. Barone, B. Mennucci, M. Cossi, G. Scalmani, N. Rega, G. A. Petersson, H. Nakatsuji, M. Hada, M. Ehara, K. Toyota, R. Fukuda, J. Hasegawa, M. Ishida, T. Nakajima, Y. Honda, O. Kitao, H. Nakai, M. Klene, X. Li, J. E. Knox, H. P. Hratchian, J. B. Cross, V. Bakken, C. Adamo, J. Jaramillo, R. Gomperts, R. E. Stratmann, O. Yazyev, A. J. Austin, R. Cammi, C. Pomelli, J. W. Ochterski, P. Y. Ayala, K. Morokuma, G. A. Voth, P. Salvador, J. J. Dannenberg, V. G. Zakrzewski, S. Dapprich, A. D. Daniels, M. C. Strain, O. Farkas, D. K. Malick, A. D. Rabuck, K. Raghavachari, J. B. Foresman, J. V. Ortiz, Q. B. Cui, A.G., S. Clifford, J. Cioslowski, B. B. Stefanov, G. Liu, A. Liashenko, P. Piskorz, I. Komaromi, R. L. Martin, D. J. Fox, T. Keith, M. A. Al-Laham, C. Y. Peng, A. Nanayakkara, M. Challacombe, P. M. W. Gill, B. Johnson, W. Chen, M. W. Wong, C. Gonzalez, J. A. Pople, *GAUSSIAN03 (Revision C.02)*, Gaussian, Inc.: Wallingford, CT, 2004.

[5] a) W. Kohn, A. D. Becke, R. G. Parr, *J. Phys. Chem.* **1996**, *100*, 12974-12980, b) A. D. Becke, *Phys Rev A* **1988**, *38*, 3098-3100.

[6] a) A. D. Mclean, G. S. Chandler, *J. Chem. Phys.* **1980**, *72*, 5639-5648, b) R. Krishnan, J. S. Binkley, R. Seeger, J. A. Pople, *J. Chem. Phys.* **1980**, *72*, 650-654.

[7] Z. Zheng, M. K. Elmkaddem, C. Fischmeister, T. Roisnel, C. M. Thomas, J.-F. Carpentier, J.-L. Renaud, *New J. Chem.* **2008**, *21*, 2150-2158.

[8] F. A. Cotton, L. M. Daniels, G. T. Jordan IV, C. A. Murillo, *Polyhedron* **1998**, *17*, 589-597.

[9] R. A. Jacobsen, J. E. Johnson, *Acta Crystallogr.* **1973**, *B29*, 1669-1674.

[10] G. J. Pyrka, A. A. Pinkerton, *Acta Crystallogr.* **1990**, *C48*, 91-94.